Received: 9 September 2020 | Revised: 18 November 2020 | Accepted: 28 November 2020

DOI: 10.1111/jvs.12976

METHODS ON VEGETATION SCIENCE

Journal of Vegetation Science IAVS

Revealing the functional traits linked to hidden environmental factors in community assembly

Valério D. Pillar[1,2,3] | Francesco Maria Sabatini[2,3] | Ute Jandt[2,3] | Sergio Camiz[1,4] | Helge Bruelheide[2,3]

[1]Department of Ecology, Universidade Federal do Rio Grande do Sul, Porto Alegre, Brazil

[2]Institute of Biology/Geobotany and Botanical Garden, Martin Luther University Halle-Wittenberg, Halle, Germany

[3]German Centre for Integrative Biodiversity Research (iDiv) Halle–Jena–Leipzig, Leipzig, Germany

[4]National Research Council – ISPC – Sciences of Cultural Heritage Institute, Roma, Italy

Correspondence
Valério D. Pillar, Department of Ecology, Universidade Federal do Rio Grande do Sul, Porto Alegre, RS, 91501-970, Brazil.
Email: vpillar@ufrgs.br

Funding information
VP was supported by the Brazilian National Research Council (CNPq grants 307689/2014-0 and 431193/2016-9) and by the *Coordenação de Aperfeiçoamento de Pessoal de Nível Superior* (CAPES PRINT/UFRGS 88887.467569/2019-00). The position of FMS at the German Centre of Integrative Biodiversity Research (iDiv) Halle–Jena–Leipzig was funded by the German Research Foundation (DFG FZT 118). SC received a CNPq visiting researcher fellowship in the framework of the Science Without Borders Programme (grant 401345/2014-9 to V.P.).

Co-ordinating Editor: David Roberts

Abstract

Aim: To identify functional traits that best predict community assembly without knowing the underlying environmental drivers.

Methods: We propose a new method based on the correlation *r*(**XY**) between two matrices of potential community composition: the matrix **X** is fuzzy-weighted by trait similarities of species, and the matrix **Y** is derived by Beals smoothing using the probabilities of species co-occurrences. Since **X** is based on one or more traits, *r*(**XY**) measures how well the traits used for fuzzy-weighting reflect the species co-occurrence patterns in **Y**. We developed an optimisation algorithm to identify the traits maximising this correlation, together with an appropriate permutational test for significance. Using metacommunity data generated by a stochastic, individual-based, spatially explicit model, we assessed the type I error and the power of our method across different simulation scenarios, varying environmental filtering parameters, number of traits and trait correlation structures. Then, we applied the method to real-world community and trait data of dry calcareous grassland communities across Germany to identify, out of 49 traits, the combination of traits that maximised *r*(**XY**).

Results: The method correctly identified the relevant traits involved in the assembly mechanisms of simulated communities, showing high power and accurate type I error. It proved to be robust against confounding aspects related to interactions between environmental factors, strength of limiting factors, and trait collinearity. In the grassland dataset, the method identified five traits that best explained community assembly. These traits reflect the size and the leaf economics spectrum, which are related to succession and resource supply, factors that may not be always measured in real-world situations.

Conclusions: Our method successfully identified the relevant traits mediating community assembly, therefore providing insights on the underlying environmental and biotic factors, even if these are hidden, unmeasured or not accessible at the spatial or temporal scale of the study.

KEYWORDS
Beals smoothing, community assembly, environmental filtering, fuzzy-weighting, hidden environmental factors, species co-occurrence, species traits

1 | INTRODUCTION

Understanding how species assemble in space and time is critical for predicting biodiversity responses to environmental change (D'Amen et al., 2017) and the effects of biodiversity losses on ecosystem processes and services (Newbold, 2018). In communities connected by dispersal, patterns of repeated co-occurrence and apparent mutual avoidance among species have often been observed (e.g. Diamond, 1975; Münzbergová and Herben, 2004). This is a consequence of the species' ecological niches and interactions, both mediated by species' morphological, physiological, phenological, or behavioural characteristics, here collectively indicated as functional traits (Keddy, 1992; McGill et al., 2006; Wilson, 2007; Götzenberger et al., 2012). These restrictions on the observed patterns constitute community assembly rules (Wilson et al., 1999).

Community assembly is driven by abiotic and biotic environmental factors favouring species with a specific set of traits. As a consequence, species co-occurrence patterns may naturally arise, because species similar with respect to these traits are expected to respond similarly to factors. Imagine an environmental factor e_1 affecting the performance (w) of species i via a trait t_1, i.e. $w_{i|t1} = f(e_1)$, or adopting a causal graph representation for the sake of simplicity: $e_1 \rightarrow t_1$. All else being equal, at a given level of e_1 some species will tend to co-occur with those having similar values of trait t_1. This will generate trait convergence for t_1 or, in other words, a trend in community-weighted means (CWMs) along changing e_1, i.e. $e_1 \rightarrow \text{CWM}_{t1}$. However, community assembly involves more complex mechanisms than that. First, the units subject to environmental filtering are whole organisms with sets of morpho-physio-phenological traits (Violle et al., 2007) which cannot be physically disentangled in response to different factors. Second, traits are often correlated, given that the multivariate trait space of species is strongly concentrated in a small number of trait value combinations, owing to coordination and trade-offs between traits as well as ecological and phylogenetic constraints (Murren, 2002; Díaz et al., 2016; Céréghino et al., 2018). As a consequence of these two constraints, a factor effect (e_1) on a trait (t_1) may depend on the value of another trait (t_2) in the same organism, either under the effect of the same factor, i.e. $e_1 \rightarrow t_1|t_2$, or another factor, i.e. $(e_1 \rightarrow t_1) \mid (e_2 \rightarrow t_2)$. In this case, one trait may be more limiting than another depending on the strength of the factor effects (Sih and Gleeson, 1995; Gorban et al., 2011). Also, unknown factors affecting t_1 will generate increased variance in t_1 along the known e_1 gradient (Kaiser et al., 1994; Thomson et al., 1996; Cade and Noon, 2003). These mechanisms may generate patterns of trait divergence (Pillar et al., 2009), e.g. when the community-weighted variance, or functional diversity (FD), of a trait increases along an environmental gradient.

But how to identify which functional traits are relevant in mediating community assembly, irrespective of whether the mechanisms lead to convergence or divergence patterns? Traditionally, these traits have been identified by relating community trait patterns to environmental conditions or resource levels, hereafter called *environmental factors* for simplicity (Pillar and Orlóci, 1993; Díaz and Cabido, 1997; Pillar, 1999; Lavorel and Garnier, 2002; Pillar et al., 2009; Bruelheide et al., 2018). This approach, however, falls short when the factors are hidden, i.e. unknown or not observable. This is the case, for instance, when the factor was simply not measured, when it is related to unknown past conditions, but also when it affects community assembly at a much finer resolution than the grain size of the studied community units. Moreover, community assembly might also depend on biotic factors related to species interactions, such as predation, facilitation, or competition. The interactions might be indirect, as in the case of a plant subtracting or adding resources to other plants, or direct, such as grazing and predation, which might filter traits related to avoidance or tolerance. Both classes of environmental factors are often difficult to measure, but are likewise expected to shape the functional profile of ecological communities (Mason and Wilson, 2006; D'Amen et al., 2017).

Under the assumption that these relevant yet hidden factors are reflected in community composition, compositional data might be analysed in a way that allows to identify the fundamental traits mediating community assembly. Once the traits are known, one can use factor–trait relations known from ecological theory or from other empirical studies (e.g. Díaz et al., 2007; Dubuis et al., 2013; Bruelheide et al., 2018) to make inferences about those factors, even if hidden, that are responsible for filtering (Keddy, 1992) species in the studied communities.

Here we propose and test a data-driven method to identify those functional traits that best predict community assembly without knowing the relevant environmental or biotic factors shaping the studied communities. The foundation of our approach is to relate two ways of predicting potential community composition to each other, either based on the probability of species co-occurrence (Beals, 1984) or using fuzzy-weighting based on species traits (Pillar et al., 2009). Given a pool of m species spread across n communities in a metacommunity (Leibold et al., 2004), Beals (1984) smoothing predicts the probability of occurrence of every species j in each community k, estimated as the weighted average of the pairwise co-occurrence probabilities of species j with those species actually present in community k. Beal smoothing has been proved to effectively recover the latent community structure in metacommunities described by noisy data (De Cáceres and Legendre, 2008; Smith, 2017). Fuzzy-weighting (Pillar et al., 2009) has some analogy to Beals smoothing but, instead

of co-occurrence probabilities, it predicts the probability of occurrence of every species in each community based on the trait similarity with those species actually present in the community. Fuzzy-weighting results in a trait-based transformation of species composition in a metacommunity. Thus, it fully describes the potential community composition regarding traits encompassing both convergence and divergence, which may reflect the environmental structure depending on the selected traits (Pillar et al., 2009). The correlation between these two matrices of predicted species composition should thus measure how well the traits used for fuzzy-weighting reflect the species co-occurrence patterns. Hence, finding the set of functional traits mediating community assembly can be reduced to the task of developing an optimisation algorithm that identifies the traits maximising this correlation, together with an appropriate permutational test for significance.

To test our method, we generated data with known environmental filtering mechanisms and analysed how often our method correctly identified the traits involved in the simulated process of community assembly. Then, we applied the method to real plant community data and checked whether it identified traits that can be considered relevant in mediating species assembly in the studied communities.

2 | METHODS

As input, the analysis uses community composition matrix **W** of sites by species, and matrix **B** of traits describing the species found in the metacommunity.

The Beals smoothing (Figure 1) requires a matrix **P** of pairwise probabilities of species co-occurrences, which is derived from **W**:

$$p(i|j) = \frac{\sum_{k=1}^{n} w_{ki}^{0} w_{kj}^{0}}{w_{j}^{0}} \quad (1)$$

where $p_{i|j}$ is the probability of species i to occur in a community when species j is present, w_{ki}^{0} and w_{kj}^{0} are the incidences (0, 1) of the species i and j in the community k, and $w_{.j}^{0}$ is the total incidence of species j across the n communities in **W**. Normalising **W** by its site totals, to compute relative species abundances ($\mathbf{W}_p$), and multiplying it by **P** (Figure 1) results in Beals-smoothed matrix **Y** of species by communities (Beals, 1984; De Cáceres and Legendre, 2008). In this definition, the target species were included for the estimation of their own probability of occurrence in a community (Beals, 1984).

For the fuzzy-weighting of the community composition in **W** (see Figure 1), the species probability of occurrence in a community is estimated based on the species' trait similarities with other species observed in the same community (Pillar et al., 2009). For this task, considering the traits in **B**, a species by species similarity matrix **S** is computed by using the Gower similarity index (ranging 0–1). By normalising the rows of **S** by their row total, a matrix **U** is obtained whose elements define self- and cross-belongings of species to fuzzy sets (Duarte et al., 2016). Each column j of **U** defines a fuzzy set of species functionally similar to species j. This way the degrees of belonging of each species across the fuzzy sets sum up to 1, though symmetry is lost, i.e. $u_{ij} \neq u_{ji}$. The closer a given species is to species j in trait space, the higher is its degree of belonging to the fuzzy set j and the better it can functionally represent the species j. The fuzzy-weighted community composition is computed by multiplying the site total standardised matrix $\mathbf{W}_p$ by **U**, resulting in a communities by species matrix **X** (Figure 1). As in $\mathbf{W}_p$ the values in **X** also add to 1 for every site, so that the species proportions may be interpreted as

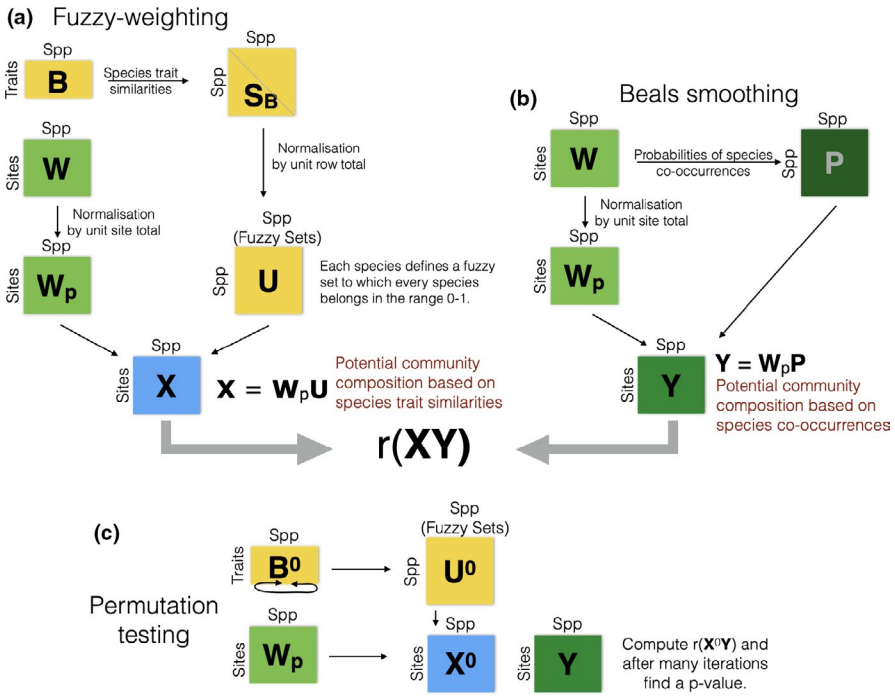

FIGURE 1 Data analysis steps for: (a) fuzzy-weighting applied to the species composition matrix **W** which, combined with the species traits in the matrix **B**, generates the matrix **X**; (b) Beals smoothing applied to **W** to generate the matrix **Y**; and (c) permutation test for the significance of the matrix correlation r(**XY**) by permuting the columns of **B** (or **U**) generating $\mathbf{B}^0$ (or $\mathbf{U}^0$) and derived $\mathbf{X}^0 = \mathbf{W}_p\mathbf{U}^0$

probabilities. While in $\mathbf{W}_p$ these probabilities refer to the species actually observed in the community, in **X** they refer to the species pool in the metacommunity. That is, each element in **X** is an estimation of the probability to find the species *j* in the community *k*, given the functional similarity of *j* to the species actually occurring in *k*.

To assess the correlation *r*(**XY**) between the matrices **X** and **Y**, we used the Rd coefficient (Omelka and Hudecová, 2013), which is a Pearson correlation coefficient of the Gower-centred pairwise distances (Gower, 1966) based on **X** and **Y**, considering the full distance matrices. The closer Rd is to 1, the higher is the association between community distances in the fuzzy-weighted species composition based on traits and those in the potential composition based on species co-occurrences. The Rd correlation *r*(**XY**) can be interpreted as the degree to which the traits used in **X** reflect co-occurrence patterns in **Y**. We chose the Rd coefficient based on Euclidean distances because, compared to the Mantel correlation or the RV coefficient (Robert and Escoufier, 1976), it can also detect non-linear relations between the matrices (Omelka and Hudecová, 2013). Note that, if squared distances were used, the Rd would coincide with the RV (Omelka and Hudecová, 2013).

2.1 | Testing for significant traits

The significance of the Rd correlation *r*(**XY**) was tested under the null hypothesis that species assembly is unrelated to species traits. This null model was originally described by Pillar et al. (2009) for testing matrix correlations between environmental variables and CWMs or fuzzy-weighted composition; it corresponds to the column-based permutation test described in Zelený (2018) for the analogous case of the community-weighted mean approach (see also Zelený and Schaffers, 2012; Duarte et al., 2018; ter Braak et al., 2018). This is achieved by keeping **W** and **Y** constant and permuting the columns of **B** (or, equivalently, of **U**) enough times to allow the computation of a probability $p[r(\mathbf{X}^0\mathbf{Y}) \geq r(\mathbf{XY})]$ (Figure 1c). If the *p*-value is not larger than an a priori fixed error probability threshold α, then *r*(**XY**) is deemed significant and we conclude that the trait or traits included in the definition of **X** has/have been relevant for community assembly in the analysed metacommunity. This permutation approach breaks all the relations between the functional trait characteristics of the species and their presence or abundance in **W**. This has the following advantages: First, it controls for the fact that the species composition (**W**) is used to derive the matrices at both sides of *r*(**XY**), thus it avoids bias that would result if permutations were done among the sites in **X** or **Y**. Second, it avoids the source of bias described by Hawkins et al. (2017) affecting aggregated measures in community analysis. Third, by keeping **W** and **Y** constant, any spatial or temporal autocorrelation in the compositional data will be incorporated in the null model, thus avoiding bias in the permutation testing (Pillar et al., 2009; Gotelli and Ulrich, 2012). Note that this approach was preferred to the max test described by ter Braak (2018), since the latter cannot be theoretically justified for testing the correlation *r*(**XY**) relating two intrinsic sample attributes (Zelený, 2018).

This permutation procedure can be repeated by considering different subsets of traits to obtain various fuzzy-weighted community composition matrices in **X**. The trait or combination of traits maximising *r*(**XY**), as long as its *p*-value is significant, is expected to be optimal for observational and experimental studies aiming at identifying traits linked to hidden environmental factors in community assembly.

To select the optimal subset of traits, for the simulated data we considered the *p*-values generated according to Figure 1c only, whereas for the real-world data we combined the permutation test with bootstrap resampling. Thus, since the real-world data are a sample, in addition to testing for significance, we calculated confidence intervals for the observed *r*(**XY**) for each trait or trait combination, and compared them across traits or trait combinations. For this task, in each bootstrap iteration, the plots were resampled with replacement to obtain a bootstrap sample, which redefined $\mathbf{X}^*$ and $\mathbf{Y}^*$ with the selected plots, used to recalculate $r(\mathbf{X}^*\mathbf{Y}^*)$. The distribution of $r(\mathbf{X}^*\mathbf{Y}^*)$ across the bootstrap samples allowed estimating the 95% confidence interval of the observed *r*(**XY**). Yet, as both **X** and **Y** are based on the same species composition **W**, they are expected to have non-zero *r*(**XY**) even if the trait combination used to build **X** plays no role in community assembly. Thus, we applied the permutational approach shown in Figure 1c to compare $r(\mathbf{X}^*\mathbf{Y}^*)$ with a possible expected correlation $r(\mathbf{X}^{*0}\mathbf{Y}^*)$ assuming the selected trait or traits has/have no role in community assembly. After a large number of bootstrap/permutation iterations, the probability $p[r(\mathbf{X}^{*0}\mathbf{Y}) \geq r(\mathbf{X}^*\mathbf{Y}^*)]$ was the proportion of iterations in which $r(\mathbf{X}^{*0}\mathbf{Y}^*)$ was larger than $r(\mathbf{X}^*\mathbf{Y}^*)$.

Finally, we used the 95% confidence intervals of each correlation *r*(**XY**) to compare and rank the trait combinations. Ideally, we would examine iteratively every trait subset with 1 to *k* traits in **B** and the corresponding significance of the resulting *r*(**XY**) to find an optimal trait subset. However, when the number of traits is large (e.g. >20), the number of possible combinations may become numerically unmanageable (e.g. 1,048,575 possible combinations for 20 traits). Here we adopted a partial stepwise algorithm to efficiently explore the space of trait combinations and reduce computation demand. The optimal trait set was then compared with the one obtained by testing all possible trait combinations. Further, we benchmarked the results with those of the analyses performed on simulated data with known assembly rules. The partial stepwise algorithm acts as follows: once computed *r*(**XY**) for each single trait, the traits resulting with significant *r*(**XY**) correlations were selected. We then repeated the procedure by considering all the pairwise combinations of traits being individually significant. If any pairwise combinations had an *r*(**XY**) significantly better than the best trait (i.e. whose 95% confidence intervals did not overlap with those of the best trait), we considered the pairwise combination having the highest and significantly better *r*(**XY**) as the new best. We then kept these two traits as fixed, while testing the effect of adding another trait, trying to find a new best. If no pairwise combination performed better than the best trait, we tested all possible three-way combinations including the initial best trait, and checked if a new best combination could be found. If no new best existed, we proceeded considering all four-way combinations, and so on. We added one trait

at a time up to the number of individually significant traits, so as to find the optimal combination of traits. This should not be seen as the absolute optimal combination of traits, but rather an optimal solution conditional on the previously selected traits. For each combination, we generated *p*-values using 999 random iterations of bootstrap/permutation plus one iteration for the observed $r(\mathbf{XY})$.

2.2 | Analyses with simulated communities

To test whether our method is able to discriminate relevant and non-relevant traits, we applied it to simulated plant community composition data. We generated data by repeatedly modelling metacommunities (sets of plant communities) based on specified assembly mechanisms in which the underlying environmental factors were known. Then, we analysed the simulated data with the above-described method to identify the traits driven by these factors. This way we could check by means of type I error and power analyses whether the relevant traits for the assembled communities were correctly revealed. We assessed type I error as the proportion of metacommunities in which neutral traits, i.e. traits not being favoured by a given set of environmental factors, were incorrectly identified as relevant. To quantify power, we calculated the proportion of metacommunities in which traits involved in the simulated assembly mechanisms were correctly identified as being significant, i.e. when the test with the simulated metacommunity resulted in $p[r(\mathbf{X}^0\mathbf{Y}) \geq r(\mathbf{XY})] \leq 0.05$. Given the low number of traits involved in the generation of the simulated data, we evaluated significance both for all traits considered individually, as well as for all possible trait combinations.

We used a stochastic, individual-based model for simulating metacommunities stepwise from a given pool of species and their functional traits (Pillar and Camiz, unpublished). At each step, the model can predict the arrival, establishment, and extinction of individuals belonging to each species, based on probability functions with specific parameters. We then analysed the metacommunity structure after a given number of years (iterations). We generated different simulated metacommunities by specifying different combinations of trait numbers, environmental filtering parameters, and species level trait correlations (Appendix S1). The other parameters were set at random. For each set of model parameters, we generated and analysed 100 simulated metacommunities.

We explored four simulation scenarios to assess whether the method can correctly identify the relevant traits in the simulated metacommunities, when confounding aspects related to correlation among traits and contrasting strengths and interactions between environmental filtering effects are in play. In the first case (Scenario 1), we generated communities assuming two environmental factors and three functional traits. The first trait t_1 was directly dependent on e_1, i.e. $e_1 \rightarrow t_1$, while t_2 related directly to e_2, i.e. $e_2 \rightarrow t_2$. An additional trait t_n was neutral with respect to the environment. The metacommunities were generated according to an increasing magnitude of $e_1 \rightarrow t_1$, obtained by varying from 0 to 0.6 the specified linear response parameters for environmental filtering, while fixing the effect of $e_2 \rightarrow t_2$ at 0.3. We used this basic scenario to explore both the effect of the interaction between the environmental factors e_1 and e_2 on t_1 (three levels: 0, 0.3, 0.5) and to explore the effect of the correlation between traits t_1 and t_2 (three levels, 0, 0.4, 0.8).

Scenario 2 was similar to the first one, but we added a third trait t_3 directly dependent on factor e_1, i.e. $e_1 \rightarrow t_3$. In this case, both traits t_1 and t_3 were affected by the same factor e_1, but while the strength of the effect $e_1 \rightarrow t_1$ varied from 0 to 0.6, the effect $e_1 \rightarrow t_3$ was fixed at 0.3. As in the first scenario, we also examined the effect of an interaction between the factors e_1 and e_2 on t_1, and of pairwise correlations between traits t_1, t_2 and t_3.

In Scenario 3, we varied the effect $e_1 \rightarrow t_1$ from 0 to 0.6, as above, but progressively including also the effect of additional environmental factors on their respective functional traits (i.e. $e_2 \rightarrow t_2$; $e_3 \rightarrow t_3$; $e_4 \rightarrow t_4$), all fixed to 0.3. In all simulations, a neutral trait t_n was added with the purpose of testing the type I error. Both factor interaction effects and pairwise trait correlations were set to zero in this scenario. We also examined a variation of this situation in Scenario 4 by setting the environmental factor effects on the last two traits ($e_3 \rightarrow t_3$; $e_4 \rightarrow t_4$) with a very weak magnitude of 0.01, to simulate an increasing number of nearly neutral traits.

We performed supplementary analyses to help understand and interpret our results. We tested whether the Rd correlation $r(\mathbf{XW})$ between fuzzy-weighted composition (**X**) and simulated species proportions in the communities ($\mathbf{W}_p$) would be able to discriminate between relevant and non-relevant traits. We did the same for the correlation $r(\mathbf{XE})$ between **X** and environmental factors (**E**) driving the simulated community assembly process. For these tests, we considered only the simulated communities described in Scenario 1. Additionally, we assessed the effect of sample size, i.e. the number of communities sampled from a metacommunity, on the power of our method to detect relevant traits for a selected case of simulated data, for both the $r(\mathbf{XY})$ and $r(\mathbf{XW})$ correlations. Furthermore, we partitioned the taxonomic diversity of our simulated data into α, β and γ components (De Bello et al., 2010), to show the effect of Beals smoothing and fuzzy-weighting on β diversity. Also, by means of Rd correlations $r(\mathbf{YE})$ and $r(\mathbf{WE})$ we assessed whether Beals smoothing (**Y**) improved the correlation between environmental structure (**E**) and community composition.

2.3 | Analyses with real communities

To test whether our method is helpful in highlighting relevant traits in a real-world dataset, we used data on dry calcareous grasslands vegetation in Germany. Such grasslands belong to the *Festuco-Brometea* class (Mucina et al., 2016) and are coded "E1.2a Semi-dry perennial calcareous grassland" in the European Red List of Habitats (Grassland Habitat Group, 2017). The dataset had been previously used in a continental survey (Willner et al., 2019). Here we analysed a subsample of 565 plots randomly taken from the original data (see map in Appendix S2), and including 488 species. We combined the compositional data (square-root-transformed percentage cover,

to reduce the excessive weight of dominant species) with the species trait information for 49 traits (Appendix S3) taken from the BIOLFLOR (Klotz et al., 2002) and TRY databases (Kattge et al., 2011, 2020). The TRY data, which included 16 traits, were gap-filled and aggregated to species mean values (Shan et al., 2012; Fazayeli et al., 2014; Schrodt et al., 2015; Bruelheide et al., 2019). Trait coverage was complete, except for pollination, leaf persistence, sclerophylly, and succulence, for which the species with functional trait information accounted for an average of at least 96.5% of the plot total cover across the plots in our sample (Appendix S3).

Based on the procedure described above we identified an optimal subset of traits, i.e. the combination of traits with the maximum relevance for the assembly of these grassland communities. Furthermore, we used principal components analysis (PCA) based on pairwise trait correlations to identify the main trends of trait variation at the species level.

To illustrate how well the selected traits reflected community composition, we applied PCA to the dry grassland data based on the covariance of Beals' smoothed community composition (matrix **Y**). We then superimposed three sets of supplementary variables on this ordination space: (a) the principal components of another PCA computed based on the covariance of fuzzy-weighted composition (matrix **X**) for the optimal traits; (b) the CWMs of all significant traits; and (c) available environmental variables. These projections were based on the Pearson correlations between the supplementary variables and the principal components of **Y**. As environmental variables, we compiled annual mean temperature and annual mean precipitation from CHELSA, V1.1 (Karger et al., 2017) and assigned these values to the plots with a 30 arcsec resolution. Also, two soil variables (soil pH and content of soil organic carbon) were extracted from the SOILGRIDS project (https://soilgrids.org/, licensed by ISRIC—World Soil Information), downloaded at 250-m resolution and then resampled using the 30 arcsec grid of CHELSA.

3 | RESULTS

3.1 | Simulated communities

In the first scenario (Figure 2, top, leftmost panel), the proportion of simulated metacommunities with a significant r(**XY**) correlation taking the trait t_1 alone expectedly increased when the factor effect e_1 on t_1 increased beyond zero, and reached 100% power with the strongest effect. However, as the effect of e_1 on t_1 increased, the power to detect a significant r(**XY**) for the trait t_2 alone was suppressed. In addition, the method correctly indicated that the proportion of simulated metacommunities with a significant r(**XY**) for t_n alone was low and close to the nominal α threshold α = 0.05,

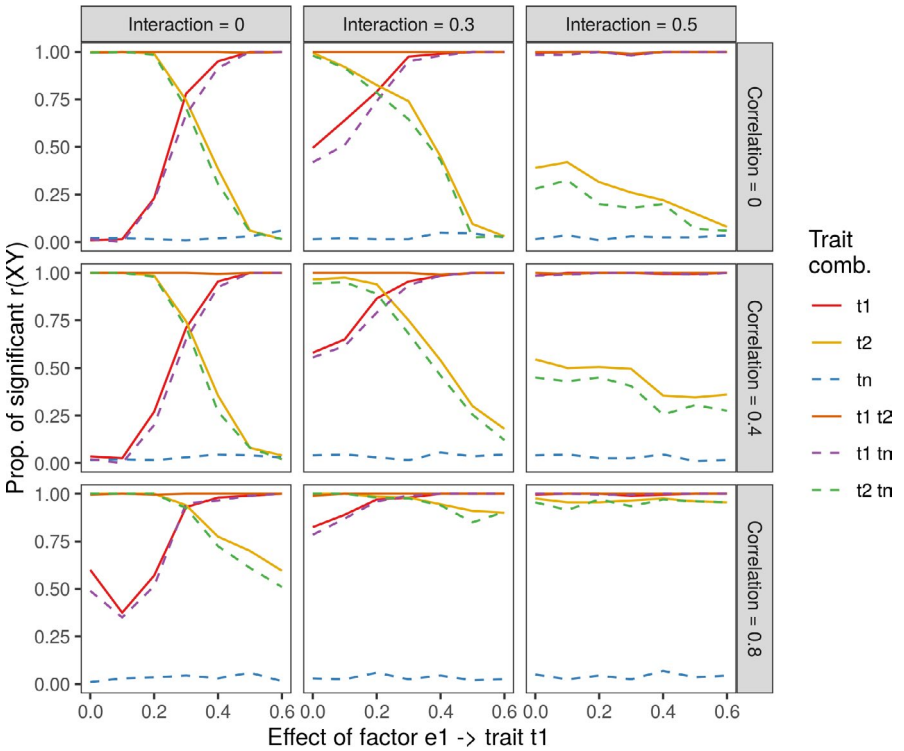

FIGURE 2 Proportion of significant Rd correlation r(**XY**) between community distances based on trait-based fuzzy-weighted (**X**) and Beals-smoothed (**Y**) species composition across simulated metacommunities with increasing strength of factor effect e_1 on trait t_1, and varying the magnitude of the $e_1 \times e_2$ interaction, and the strength of the pairwise correlations between traits t_1 and t_2 (Scenario 1). The vertical axis indicates the proportion of simulated metacommunities for which the p-value for r(**XY**) found by permutation was not larger than the threshold α = 0.05. The graphics show traits considered individually and different trait combinations defining fuzzy-weighted species composition. Further details on the set of parameters for community assembly simulations and summary statistics for some simulated data are in Appendix S1. Dashed lines represent combinations of traits including the neutral trait (t_n)

i.e. the type I error was not inflated. However, considering combinations of traits, we found that all two-trait combinations involving the neutral trait t_n returned significant r(**XY**) at similar power to the one obtained when considering traits t_1 or t_2 alone. This is clearly misleading considering that t_n was not under environmental filtering in community assembly. We took this result as evidence for the need to test only combinations of traits which produced a significant r(**XY**) when taken individually.

Furthermore, as the effect of factor interaction $e_1 \times e_2$ on trait t_1 increased (Figure 2, top panels), the relevance of t_1 was high irrespective of how low the factor effect e_1 was on the same trait. The power to detect a significant r(**XY**) for t_2 alone was even more strongly suppressed with increasing interaction $e_1 \times e_2$ on trait t_1 (Figure 2, mid and right column of panels). However, when the correlation between t_1 and t_2 increased (Figure 2, mid and bottom panels), the suppression of t_2 by t_1 was weakened.

The effect of suppression between traits can be better examined in the second scenario (see results in Appendix S4). Similarly to what was shown in Figure 2, in the absence of factor interaction and trait correlation the detection of the trait t_2 as relevant in community assembly was progressively suppressed by t_1 when the filtering effect of factor e_1 increased. However, t_3, which in this scenario is filtered by the same factor e_1, was very little suppressed while the filtering effect on t_1 increased, i.e. became more limiting for the establishment and the survival of plant individuals. Yet, under increasing strength of the interaction $e_1 \times e_2$ on t_1, the power to detect a significant r(**XY**) for t_3 alone decreased. Further, similar to the first scenario, the pairwise correlation increase at

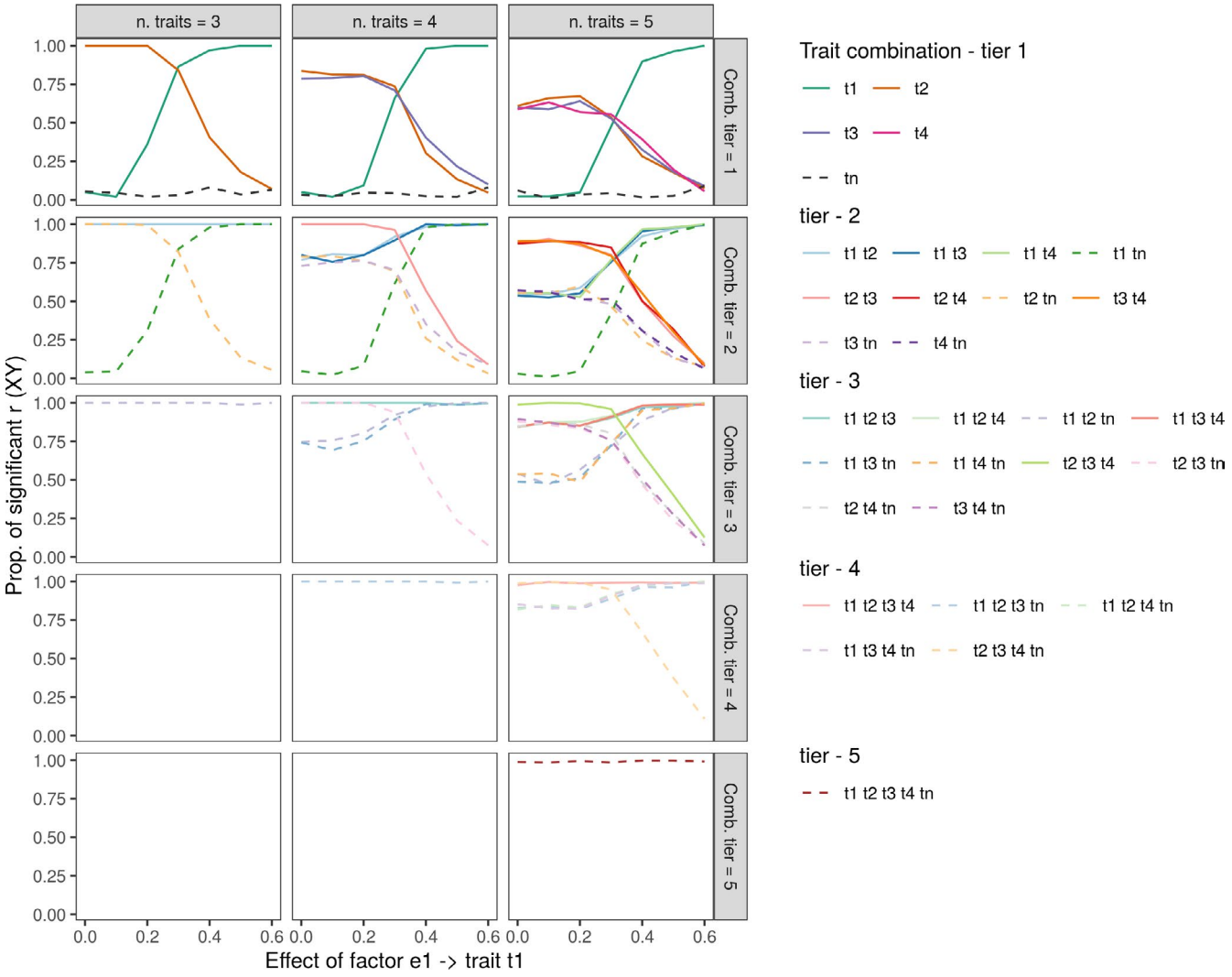

FIGURE 3 Proportion of significant Rd correlation r(**XY**) between community distances based on trait-based fuzzy-weighted (**X**) and Beals-smoothed (**Y**) species composition across simulated metacommunities with increasing strength of factor effect e_1 on trait t_1, and increasing the number of traits used in simulating metacommunities (Scenario 3). The vertical axis indicates the proportion of simulated metacommunities for which the p-value found by permutation was not larger than the threshold $\alpha = 0.05$. The number of traits ranged from 3 to 5 (left to right panels), with one trait t_n always being neutral. Traits are either shown individually (top row), or in combinations (from two to five, top to bottom rows) to improve visualization. Dashed lines represent combinations of traits including the neutral trait (t_n)

the species level between t_1, t_2 and t_3 reduced such a suppression effect. As before, the type I error was not inflated regarding the neutral trait t_n taken alone.

In the third scenario, we analysed whether the performance of our method is influenced by the number of traits involved in community assembly (Figure 3). The simulations based on three traits generated power graphs with a similar pattern compared to those based on four or five traits. In all cases, the trait t_1 was filtered under increasing factor effect e_1, t_n was always neutral, and the other traits were under a fixed, intermediate factor effect. As in Figure 2, the analysis of the *r*(**XY**) using trait combinations including the neutral trait t_n would be as relevant as using the other non-neutral traits alone. The results of the simulations performed under the conditions set for the fourth scenario indicated that neutral traits were equally non-significant irrespective of the increasing number of neutral traits (Appendix S5).

The supplementary analyses with data simulated under the same scenario as used in Figure 2 indicated that the power for detecting knowingly significant traits was consistently higher when using the correlation *r*(**XY**) compared to *r*(**XW**) (Figure 2 vs. Appendix S6a). Also, the power for detecting knowingly significant traits by the correlation *r*(**XE**) showed a steep increase at very low levels of factor effect e_1, but for intermediate or stronger effect levels the power of *r*(**XE**) was similar to *r*(**XY**) (Appendix S6b). As expected, the correlation *r*(**XE**) based on t_2 remained non-significant, except when t_2 was highly correlated with t_1. Further, the power to detect a significant correlation *r*(**XY**) correlation was affected only when samples with less than 50 communities were used, and the drop in the power was steeper for correlation *r*(**XW**) (Appendix S7). Eventually, it was clear that Beals smoothing strongly reduced proportional beta diversity in the composition matrix (Appendix S8). The same was observed for fuzzy-weighting (results not shown). Despite the homogenising effect, the correlation between community patterns and environmental structure was not only preserved but enhanced by Beals smoothing, and this was not affected by sample size, at least for the range of simulated conditions we considered (Appendix S8).

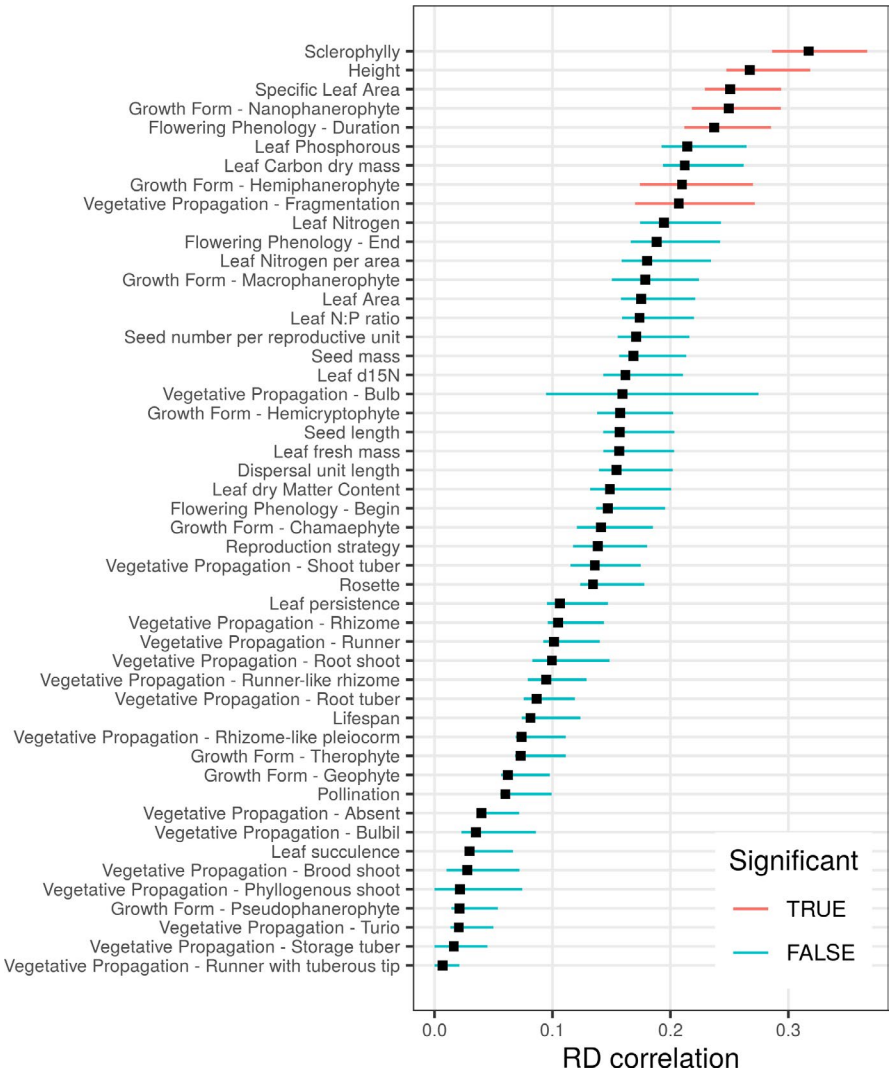

FIGURE 4 The Rd correlation *r*(**XY**) between community distances based on trait-based fuzzy-weighted (**X**) and Beals-smoothed (**Y**) species composition, when considering one trait at a time. The observed *r*(**XY**) was deemed significant (at *p*-value ≤ 0.05, one-sided) when it was greater than the corresponding correlation coefficient calculated using permuted species traits in at least 95% of the bootstrap samples. The segments represent the 95% bootstrap confidence intervals of the observed *r*(**XY**); in red are the traits with significant *r*(**XY**), in blue are the non-significant ones

3.2 | Real communities

While applying the same approach to dry calcareous grasslands, seven out of the 49 traits returned a significant *r*(**XY**) when taken one by one: sclerophylly, plant height, specific leaf area (SLA), nanophanerophyte and hemiphanerophyte growth-forms, flowering duration, and vegetative propagation through fragmentation. Taken singularly, sclerophylly was the trait that best explained community assembly (Figure 4).

By using the partial stepwise algorithm, the iterative increase of the number of traits used to calculate the matrix **X** resulted in a progressive increase in *r*(**XY**), although the confidence intervals of the regression coefficients were mostly overlapping (Figure 5). When considering pairwise combinations of traits, sclerophylly combined with flowering duration returned a significantly higher *r*(**XY**) than sclerophylly alone. There were no three- and four-way combinations of traits significantly improving the *r*(**XY**) compared to the sclerophylly/flowering duration pair (for details see Appendix S9). Only when considering five traits together, the improvement of *r*(**XY**) became significant: besides sclerophylly and flowering duration, the other traits composing this combination of traits were plant height, SLA, and propagation by fragmentation. We assumed this as being the optimal combination of traits for predicting fuzzy-weighted species composition related to species co-occurrences, as no additional increase in dimensionality resulted in a significant improvement of *r*(**XY**) (Figure 5). This same subset of traits was found as best by testing all the 127 combination of the seven significant traits (results not shown).

The PCA of the trait correlations at the species level (Appendices S10, S11) revealed two main axes of independent trait variation, one reflecting the leaf economics spectrum (SLA vs. sclerophylly), which was also associated with the hemiphanerophyte growth form and the propagation by fragmentation, and the other the size spectrum (plant height), which was also associated with the nanophanerophyte growth form and the flowering duration. However, uncorrelated traits at species level were not necessarily also uncorrelated at community level. For example, while at species level plant height was uncorrelated to sclerophylly ($r = -0.06$) and fragmented vegetative propagation ($r = -0.07$), their corresponding CWM values showed considerable Pearson correlations (−0.44 and 0.31, respectively; Appendix S12).

The five traits that were identified as the most relevant ones (Figure 5), and the so defined principal components of fuzzy-weighted composition (FW-PCs, Appendix S13) reflected different dimensions (PCs) of Beals-smoothed community composition, as shown in Figure 6 (see correlations in Appendix S14). FW-PC1 reflected the leaf economics spectrum (SLA vs. sclerophylly) and was correlated also to PC1 but mostly to PC3 of the Beals-smoothed community composition (11.2% of total variation). FW-PC2 reflected an increasing representation of the nanophanerophyte growth form vs. decreasing flowering duration and was mostly correlated to the first principal component (PC1) of the Beals-smoothed community composition (27.7% of total variation). FW-PC3 was only (weakly) correlated to PC4 but did not reflect any trait in particular. Yet, the links between the FW-PCs, the traits and the PCs of the Beals-smoothed community composition become clearer by examining the two-dimensional ordination spaces. In the space defined by PC1 and PC2, two diagonal axes may be identified, one reflecting FW-PC1 and the other FW-PC2, both representing different traits. The size spectrum (height) was captured by both FW-PC1 and FW-PC2. Finally, the available potential environmental predictors presented weak correlations with the first four principal components, being highest for mean annual precipitation (−0.386 with PC1, Figure 6, Appendix S14).

4 | DISCUSSION

How to identify those functional traits mediating community assembly when relevant environmental factors are unknown? Answering this question is crucial to improve our predictions on how ecological assemblages will change in the face of global change (Newbold, 2018). Here, we developed a method to identify the functional traits mediating community assembly, which does not rely on measuring the actual environmental gradients ultimately driving it. Our approach relies on the comparison of two alternative ways of predicting

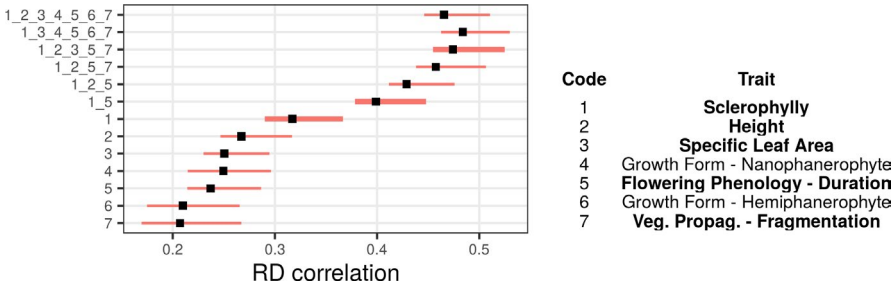

FIGURE 5 Rd correlation *r*(**XY**) (black squares) and confidence interval (red lines) between community distances based on trait-based fuzzy-weighted (**X**) and Beals-smoothed (**Y**) species composition, when progressing in tiers (bottom to top) based on a selected subset of traits. Only the seven significant traits defining fuzzy-weighting alone (see Figure 4) are represented. For each tier, we tested the effect of adding a new trait to the best combination of the previous tier, and only show the best result. Identical results were found by examining every combination of the seven traits. We used thick lines for traits or trait combinations providing a significant ($p \leq 0.05$) improvement with respect to the best solution at the previous tier(s). Detailed results are shown in Appendix S9

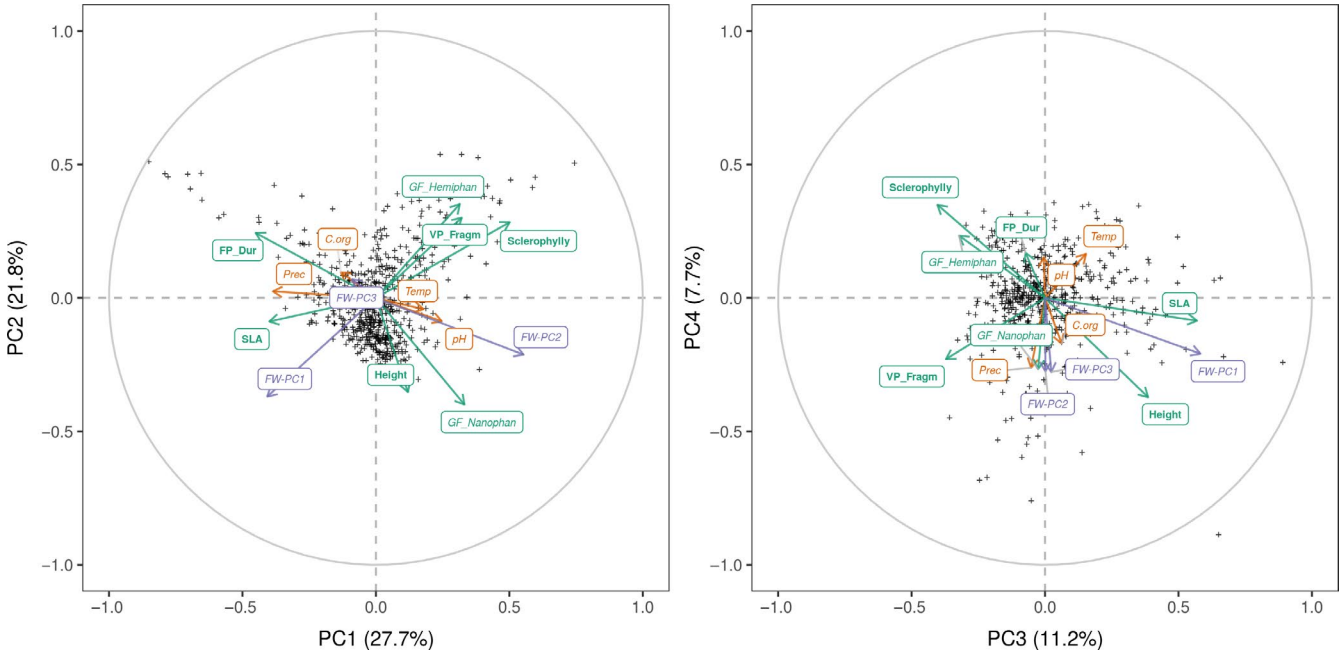

FIGURE 6 Principal components analysis of dry grassland plots based on the species variance–covariance matrix of Beals' smoothed composition (**Y** matrix). The communities (plots) are shown as cross symbols with the scores multiplied by a constant to fit into the −1 to +1 range. The community-weighted means (CWMs) for the traits with a significant Rd correlation *r*(**XY**) in Figure 4, in green, the principal components based on the fuzzy-weighted composition defined by these traits (FW-PC1, -PC2, -PC3, Appendix S13), in purple, and four environmental variables, in orange, are superimposed according to their Pearson correlations with the PCA axes (see correlations in Appendix S14). The five traits identified in Figure 5 as the best combination of traits are shown in bold green fonts. See Appendix S15and S16 for the scatterplots with the species.

species composition: Beals' smoothing of species co-occurrences probability (Beals, 1984) and fuzzy-weighting of functional traits (Pillar et al., 2009). The method comes with an optimisation algorithm able to efficiently explore the trait combination space, and derives unbiased significance values and confidence intervals using permutation and bootstrap resampling, respectively.

The results with the simulated data show that our method can identify the most relevant trait combinations mediating the assembly of biological communities along gradients. Weak trait–environment links may give low power to detect a relevant trait. However, the power of our analysis quickly increased to 100% when the magnitude of the main environmental filtering effect was greater than 0.3; the effect was specified as a linear parameter relating the factor to the expected trait values at the community level in the metacommunity model that generated the data. This suggests that the method might be sensitive enough to detect the most important traits related to discriminant environmental factors in real-world situations. Furthermore, in the simulations our approach proved sufficiently robust against the inclusion of non-relevant traits, the type I error always being close to the nominal levels, as well as against confounding factors related to interactions between environmental gradients, and correlation among traits.

However, the results with the simulated data also indicated that only those traits found to be significant when taken individually should be retained in the analysis and tested in combination with other equally relevant ones. In other words, the consideration of correlation and *p*-values per se is not sufficient to discriminate trait combinations that include irrelevant traits. For the real data, we solved this problem by using bootstrap to calculate the confidence intervals of our matrix correlation coefficients, and by adopting a partial stepwise algorithm only considering combinations of traits that were relevant when taken individually. This way, we could reliably ascertain that a combination of, e.g., two traits was significantly better than any of the two traits taken singularly. And yet, our optimisation algorithm remained sufficiently flexible to be adapted to situations under which the examination of every combination of relevant traits would be unfeasible.

Our results using simulated metacommunity data demonstrated a suppression effect among traits mediating community assembly, suggesting that traits under stronger filtering effects tend to mask traits weakly filtered. We argue that the suppression effect is not an artefact of our method of analysis, because suppression may arise in community assembly from the obvious fact that the units being filtered are not traits but whole organisms, whose traits cannot be physically disentangled according to trait responses to different factors. Under such filtering effect, the most limiting trait (Sih and Gleeson, 1995; Gorban et al., 2011) likely suppresses less limiting traits. However, suppression is stronger between traits that are filtered by different, independent environmental factors than between traits that are filtered by the same factor. Correlation among traits, contrastingly, reduces such suppression effects. We note, however, that assessing whether a trait is found non-significant for

having a weak effect or because it is suppressed by another, strongly filtered trait, is only possible when dealing with simulated data, but not in real-world applications. The opposite is also true, i.e. a trait, although significant, might not be mediating community assembly, but simply be highly correlated to another, unknown trait that is the crucial one for the species' success or failure in the communities. These problems, however, are common to most observational approaches, where causality can only be inferred, but never ascertained.

Models are useful but offer simplified representations of real systems. Thus, models should always be compared with or complemented by the analysis of real data (Noy-Meir and van der Maarel, 1987). We believe this approach was successful here. While there is no way to disentangle all the environmental factors that drive the community composition of the whole range of dry calcareous grasslands in our study system, the identification of the five most relevant traits allows some conclusions on the underlying processes. Three of the five traits are part of the two main spectra of global plant forms and functions at the species level (Díaz et al., 2016). While plant height reflects the size spectrum, SLA and sclerophylly represent the leaf economics spectrum (Wright et al., 2004).

On the one hand, plant height points to management as a key factor in community assembly of dry grasslands. Indeed, abandonment of grazing and mowing favours tall grasses, shrubs and trees. Taller species indicate ongoing secondary succession, which is a major threat for dry grasslands (Kahmen and Poschlod, 2004; Burrascano et al., 2016). We found that the successional gradient is reflected by the first and second ordination dimensions of the fuzzy-weighted composition based on the five key traits: this supports the outcomes of experiments that revealed land-use intensity and time since abandonment as main drivers of trait composition of dry grasslands (Moog et al., 2002). On the other hand, the leaf economics spectrum, characterised by SLA vs. sclerophylly (Wright et al., 2004), forms a second gradient, yet not completely independent from the successional one. In our communities, the ability to propagate through fragmentation coincides with the leaf economics spectrum gradient because this trait is represented in slow-growing perennial species fragmenting with age. In dry grasslands, the leaf economics spectrum reflects the gradient in both nutrient and water supply, along which different communities, alliances and orders are distinguished (Royer, 1991; Jandt, 1999; Willner et al., 2019). However, the overall nutrient availability, especially of N and P, in these grasslands is low, making them rather stressful habitats, home to many specialist species adapted to these specific conditions (Gilbert et al., 2009; Ceulemans et al., 2011), which favour the hemiphanerophytic life form (i.e. resting buds are situated on woody shoots).

These explanations might give the impression that the five key traits follow clear environmental gradients of easily measurable variables, yet the real-world situation is much more complex. While to some degree the plant height and leaf economics spectra follow macroclimatic gradients and result in different species pools of dry grasslands (see the map of the species pools in Bruelheide et al., 2020), microclimate might strongly deviate from macroclimate (Bruelheide and Jandt, 2007; Burrascano et al., 2013). Similarly, topographic conditions and soil depth have strong impacts on water availability, resulting in small-scale variation of communities (Leuschner, 1989). This is illustrated by one of our five traits of the optimal combination, that is flowering period duration. The CWM of this trait was neither correlated with the community trends related to height nor to the leaf economics spectrum. This is consistent with the results reported by Bouchet et al. (2017): while flowering period duration showed a strong relationship to community trait composition, it was not related to successional age. We would assume that flower duration indicates a combination of environmental factors that are usually hidden behind the main effects of these factors. Flower production depends on the availability of resources and is supported by warm and wet conditions (Craine et al., 2012). These conditions occur in early successional stages with an open vegetation structure where deeper soils provide an above-average resource supply. In the space of the traits, these particular micro-environmental conditions would promote a combination of low-stature growth close to the ground (small height) with acquisitive leaf traits (high SLA), to both of which flower period duration was moderately related.

While microclimate and soil depth are measurable, other additional factors adding to the complexity of dry grassland community assembly are not. In particular, historical factors are hidden in the present-day community assembly. For example, traditional shepherding between the 15th and 20th centuries has strongly affected the species composition of the calcareous grasslands (Poschlod and WallisDeVries, 2002). There might be further hidden factors driving the community trait composition, about which we can only speculate. For example, resource supply in dry calcareous grasslands may vary at very fine scales (Regan et al., 2014). This is both caused by a large variation of microsite soil conditions at small distances and by heterogeneous effects of grazing. Overall, it becomes apparent that, in real-world situations, community composition is not driven by a single trait–environment relation, but by a complex of different traits that are only partly related to known environmental factors.

It is worth keeping in mind the assumptions our method relies on, which is that both Beals smoothing and fuzzy-weighting of functional traits can reliably predict potential community composition. If these conditions do not hold for a given dataset, then it is likely that the $r(\mathbf{XY})$ correlation will not be significant. How predictive fuzzy-weighting of potential species composition is will depend only on the defining traits, so a careful initial selection of traits is crucial. As for Beals smoothing, it may be unreliable at extremely low beta diversity when each species is present in nearly every community in the set (McCune, 1994), at extremely high beta diversity when very few communities share species (Smith, 2017), or when the sample is very small or with very few species, or with a large proportion of species occurring at random (De Cáceres and Legendre, 2008). Thus, a non-significant $r(\mathbf{XY})$ correlation may indicate that the traits are actually not relevant, that the dataset does not meet adequately the conditions for Beals smoothing, or that the sample is too small. In this regard, the Beals test (De Cáceres and Legendre, 2008) may be helpful to identify which species in a given dataset may have their potential occurrences

reliably predicted by Beals smoothing, but whether only these species should be further retained is open to further research. A possible concern is that both fuzzy-weighting and Beals smoothing sharply reduce beta diversity in the composition matrix, but our results indicate that in this process existing community patterns reflecting the environmental structure are preserved (see also Smith, 2017 for the case of Beals smoothing).

Although trait divergence patterns may also arise in community assembly (Mason and Wilson, 2006; Wilson, 2007; Pillar et al., 2009), we did not examine the ability of our method to faithfully reveal relevant traits linked to biotic and/or abiotic factors causing trait divergence in the simulated community assembly. Yet, as the fuzzy-weighting adopted in our method integrates trait similarities at the species level fully into the community level, by means of the matrix **X** of species composition (Pillar et al., 2009), we expected that relevant traits would be revealed irrespective of the actual mechanism, whether it generated trait convergence, trait divergence or both.

The method we propose here successfully identified the relevant traits mediating community assembly, without relying on the measurement of the environmental factors responsible for the restrictions imposed on the species co-occurrence patterns. Trait–environment relations affecting community assembly (Keddy, 1992; Wilson et al., 1999; Götzenberger et al., 2012) leave persisting marks in the patterns of species co-occurrences. These marks are revealed by our approach. Considering that individuals within species tend to be more similar to each other than between species (Kazakou et al., 2014; Siefert et al., 2015), by relating species traits to species co-occurrence in communities, our method is able to identify the traits most likely affected by those trait–environment relations, even when the environmental factors are hidden, unknown, or not easily measurable. Even when environmental data are available to evaluate their correlation with functional traits, our method can identify hidden factors linked to traits unrelated to the available environmental factors. If in this case hidden factors are not found beyond the observed ones, we suggest that the right environmental factors may have been used to analyse the data. Going beyond the reliance on measured environmental factors, our method is particularly promising in those domains where obtaining a set of consistent and comprehensive environmental measurements is unfeasible. We think specifically of analysing large biodiversity databases of co-occurrence data (Bruelheide et al., 2018, 2019), where the use of our method might be instrumental to reveal the key traits underlying the geographical distribution of ecological communities, so as to better infer the key ecological gradients behind these patterns.

ACKNOWLEDGEMENTS

This paper was mostly developed during a research visit of VP to the German Centre for Integrative Biodiversity Research (iDiv) Halle–Jena–Leipzig and Martin Luther University Halle-Wittenberg. In our analyses we used the iDiv High-Performance Computing (HPC) cluster, for which we in particular acknowledge the support of Christian Krause. The provision of species trait data by the BIOLFLOR and TRY databases is acknowledged. We thank Miquel De Cáceres and Rob Smith for helpful comments. Open access funding was enabled and organized by Project DEAL.

AUTHOR CONTRIBUTIONS

VP conceived the method, with contributions by SC and HB; VP and SC devised and implemented the metacommunity simulation model; VP and FMS implemented computation tools and performed the analyses. UJ curated the dry grassland data. All authors discussed the results and contributed to the manuscript.

DATA AVAILABILITY STATEMENT

The metacommunity simulation model and the power and type I error analyses are implemented in the package SYNCSA, available at http://ecoqua.ecologia.ufrgs.br/SYNCSA.html. The R script used for the analysis of the grassland data is available at https://git.idiv.de/sPlot/hidden. The dry grassland vegetation plot data were extracted from the GVRD database available at https://www.givd.info/ID/EU-DE-014, and the sampled relevés are those listed in Appendix S16.

ORCID

Valério D. Pillar https://orcid.org/0000-0001-6408-2891
Francesco Maria Sabatini https://orcid.org/0000-0002-7202-7697
Sergio Camiz https://orcid.org/0000-0002-2566-5207
Helge Bruelheide https://orcid.org/0000-0003-3135-0356

REFERENCES

Beals, E.W. (1984) Bray-Curtis ordination: an effective strategy for analysis of multivariate ecological data. *Advances in Ecological Research*, 14, 1–55.

Bouchet, D.C., Cheptou, P.-O. and Munoz, F. (2017) Mowing influences community-level variation in resource-use strategies and flowering phenology along an ecological succession on Mediterranean road slopes. *Applied Vegetation Science*, 20, 376–387. https://doi.org/10.1111/avsc.12311

Bruelheide, H. et al. (2020) Deriving site-specific species pools from large databases. *Ecography*, 43, 1215–1228. https://doi.org/10.1111/ecog.05172

Bruelheide, H., Dengler, J., Jiménez-Alfaro, B., Purschke, O., Hennekens, S.M., Chytrý, M. et al. (2019) sPlot – A new tool for global vegetation analyses. *Journal of Vegetation Science*, 30, 161–186. https://doi.org/10.1111/jvs.12710

Bruelheide, H., Dengler, J., Purschke, O., Lenoir, J., Jiménez-Alfaro, B., Hennekens, S.M. et al. (2018) Global trait–environment relationships of plant communities. *Nature Ecology & Evolution*, 2, 1906–1917. https://doi.org/10.1038/s41559-018-0699-8

Bruelheide, H. and Jandt, U. (2007) The relationship between dry grassland vegetation and microclimate along a west-east gradient in Central Germany. *Hercynia*, 40, 153–176.

Burrascano, S., Chytrý, M., Kuemmerle, T., Giarrizzo, E., Luyssaert, S., Sabatini, F.M. et al. (2016) Current European policies are unlikely to jointly foster carbon sequestration and protect biodiversity. *Biological Conservation*, 201, 370–376. https://doi.org/10.1016/j.biocon.2016.08.005

Burrascano, S., Anzellotti, I., Carli, E., Del Vico, E., Facioni, L., Pretto, F. et al. (2013) Drivers of beta-diversity variation in Bromus erectus

semi-natural dry grasslands. *Applied Vegetation Science*, 16, 404–416. https://doi.org/10.1111/avsc.12021

Cade, B.S. and Noon, B.R. (2003) A gentle introduction to quantile regression for ecologists. *Frontiers in Ecology and the Environment*, 1, 412–420. https://doi.org/10.1890/1540-9295(2003)001[0412:AGITQR]2.0.CO;2

Céréghino, R., Pillar, V.D., Srivastava, D.S., Omena, P.M., MacDonald, A.A.M., Barberis, I.M. et al. (2018) Constraints on the functional trait space of aquatic invertebrates in bromeliads. *Functional Ecology*, 1–13, https://doi.org/10.1111/1365-2435.13141

Ceulemans, T., Merckx, R., Hens, M. and Honnay, O. (2011) A trait-based analysis of the role of phosphorus vs. nitrogen enrichment in plant species loss across North-west European grasslands. *Journal of Applied Ecology*, 48, 1155–1163. https://doi.org/10.1111/j.1365-2664.2011.02023.x

Craine, J.M., Wolkovich, E.M., Gene Towne, E. and Kembel, S.W. (2012) Flowering phenology as a functional trait in a tallgrass prairie. *New Phytologist*, 193, 673–682. https://doi.org/10.1111/j.1469-8137.2011.03953.x

D'Amen, M., Rahbek, C., Zimmermann, N.E. and Guisan, A. (2017) Spatial predictions at the community level: from current approaches to future frameworks. *Biological Reviews*, 92, 169–187. https://doi.org/10.1111/brv.12222

De Bello, F., Lavergne, S., Meynard, C.N., Lepš, J. and Thuiller, W. (2010) The partitioning of diversity: showing Theseus a way out of the labyrinth. *Journal of Vegetation Science*, 21, 992–1000. https://doi.org/10.1111/j.1654-1103.2010.01195.x

De Cáceres, M. and Legendre, P. (2008) Beals smoothing revisited. *Oecologia*, 156, 657–669. https://doi.org/10.1007/s00442-008-1017-y

Diamond, J.M. (1975) Assembly of species communities. In: Diamond, J.M. and Cody, M.L. (Eds.) *Ecology and Evolutions of Communities*. Cambridge: Harvard University Press, pp. 342–444.

Díaz, S., Kattge, J., Cornelissen, J.H.C., Wright, I.J., Lavorel, S., Dray, S. et al. (2016) The global spectrum of plant form and function. *Nature*, 529, 167–171. https://doi.org/10.1038/nature16489

Díaz, S., Lavorel, S., McIntyre, S., Falczuk, V., Casanoves, F., Milchunas, D.G. et al. (2007) Plant trait responses to grazing? A global synthesis. *Global Change Biology*, 13, 313–341. https://doi.org/10.1111/j.1365-2486.2006.01288.x

Díaz, S. and Cabido, M. (1997) Plant functional types and ecosystem function in relation to global change. *Journal of Vegetation Science*, 8, 463–474. https://doi.org/10.2307/3237198

Duarte, L.D.S., Debastiani, V.J., Carlucci, M.B. and Diniz-Filho, J.A.F. et al. (2018) Analyzing community-weighted trait means across environmental gradients: should phylogeny stay or should it go? *Ecology*, 99, 385–398. https://doi.org/10.1002/ecy.2081

Duarte, L.D.S., Debastiani, V.J., Freitas, A.V.L. and Pillar, V.D. (2016) Dissecting phylogenetic fuzzy weighting: theory and application in metacommunity phylogenetics. *Methods in Ecology and Evolution*, 7, 937–946. https://doi.org/10.1111/2041-210X.12547

Dubuis, A., Rossier, L., Pottier, J., Pellissier, L., Vittoz, P. and Guisan, A. (2013) Predicting current and future spatial community patterns of plant functional traits. *Ecography*, 36, 1158–1168. https://doi.org/10.1111/j.1600-0587.2013.00237.x

Fazayeli, F., Banerjee, A., Kattge, J., Schrodt, F. and Reich, P.B. (2014) Uncertainty quantified matrix completion using Bayesian Hierarchical Matrix factorization. In: Chen, X-w., Qu, G., Angelov, P., Ferri, C., Lai, J-h., and Arif Wani, M. (Eds.) *13th International Conference on Machine Learning and Applications (ICMLA)*. Detroit, USA: CPS (Conference Publishing Services), pp. 312–317.

Gilbert, J., Gowing, D. and Wallace, H. (2009) Available soil phosphorus in semi-natural grasslands: Assessment methods and community tolerances. *Biological Conservation*, 142, 1074–1083. https://doi.org/10.1016/j.biocon.2009.01.018

Gorban, A.N., Pokidysheva, L.I., Smirnova, E.V. and Tyukina, T.A. (2011) Law of the minimum paradoxes. *Bulletin of Mathematical Biology*, 73, 2013–2044. https://doi.org/10.1007/s11538-010-9597-1

Gotelli, N.J. and Ulrich, W. (2012) Statistical challenges in null model analysis. *Oikos*, 121, 171–180. https://doi.org/10.1111/j.1600-0706.2011.20301.x

Götzenberger, L., de Bello, F., Bråthen, K.A., Davison, J., Dubuis, A., Guisan, A. et al. (2012) Ecological assembly rules in plant communities-approaches, patterns and prospects. *Biological Reviews*, 87, 111–127. https://doi.org/10.1111/j.1469-185X.2011.00187.x

Gower, J.C. (1966) Some distance properties of latent root and vector methods used in multivariate analysis. *Biometrika*, 53, 325–338.

Grassland Habitat Group (2017) E1.2a Semi-dry perennial calcareous grassland. Available at https://forum.eionet.europa.eu/european-red-list-habitats/library/terrestrial-habitats/e.-grasslands/e1.2a-semi-dry-perennialcalcareous-grassland-1/

Hawkins, B.A., Leroy, B., Rodríguez, M.Á., Singer, A., Vilela, B., Villalobos, F. et al. (2017) Structural bias in aggregated species-level variables driven by repeated species co-occurrences: a pervasive problem in community and assemblage data. *Journal of Biogeography*, 44, 1199–1211. https://doi.org/10.1111/jbi.12953

Jandt, U. (1999) Kalkmagerrasen am Südharzrand und im Kyffhäuser. *Dissertationes Botanicae*, 322, 1–246.

Kahmen, S. and Poschlod, P. (2004) Plant functional trait responses to grassland succession over 25 years. *Journal of Vegetation Science*, 15, 21–32. https://doi.org/10.1111/j.1654-1103.2004.tb02233.x

Kaiser, M.S., Speckman, P.L. and Jones, J.R. (1994) Statistical models for limiting nutrient relations in inland waters. *Journal of American Statistical Association*, 89, 410–423. https://doi.org/10.1080/01621459.1994.10476763

Karger, D.N., Conrad, O., Böhner, J., Kawohl, T., Kreft, H., Wilber Soria-Auza, R. et al. (2017) Climatologies at high resolution for the earth's land surface areas. *Scientific Data*, 4, 170122. https://doi.org/10.1038/sdata.2017.122

Kattge, J., Bönisch, G., Díaz, S., Lavorel, S., Colin Prentice, I., Leadley, P. et al. (2020) TRY plant trait database – enhanced coverage and open access. *Global Change Biology*, 26, 119–188. https://doi.org/10.1111/gcb.14904

Kattge, J., Díaz, S., Lavorel, S., Prentice, I.C., Leadley, P. and Bönisch, G. et al. (2011) TRY–a global database of plant traits. *Global Change Biology*, 17, 2905–2935.

Kazakou, E., Violle, C., Roumet, C., Navas, M.-L., Vile, D., Kattge, J. et al. (2014) Are trait-based species rankings consistent across data sets and spatial scales? *Journal of Vegetation Science*, 25, 235–247. https://doi.org/10.1111/jvs.12066

Keddy, P.A. (1992) Assembly and response rules: two goals for predictive community ecology. *Journal of Vegetation Science*, 3, 157–164.

Klotz, S., Kühn, I. and Durka, W. (2002) *Biolflor: eine Datenbank mit biologisch-ökologischen Merkmalen zur Flora von Deutschland*. Bundesamt üur Naturschutz.

Lavorel, S. and Garnier, E. (2002) Predicting changes in community composition and ecosystem function from plant traits: revisiting the Holy Grail. *Functional Ecology*, 16, 545–556.

Leibold, M.A., Holyoak, M., Mouquet, N., Amarasekare, P., Chase, J.M., Hoopes, M.F. et al. (2004) The metacommunity concept: a framework for multi-scale community ecology. *Ecology Letters*, 7, 601–613.

Leuschner, C. (1989) Zur Rolle von Wasserverfügbarkeit und Stickstoffangebot als limitierende Standortsfaktoren in verschiedenen basiphytischen Trockenrasen-Gesellschaften des Oberelsaß, Frankreich. *Phytocoenologia*, 18, 1–54.

Mason, N.W.H. and Wilson, J.B. (2006) Mechanisms of coexistence in a lawn community: mutual corroboration between two independent assembly rules. *Community Ecology*, 7, 109–116. https://doi.org/10.1556/ComEc.7.2006.1.11

McCune, B. (1994) Improving community analysis with the Beals smoothing function. *Écoscience*, 1, 82–86. https://doi.org/10.1080/11956860.1994.11682231

McGill, B.J., Enquist, B., Weiher, E. and Westoby, M. (2006) Rebuilding community ecology from functional traits. *Trends in Ecology & Evolution*, 21, 178–185.

Moog, D., Poschlod, P., Kahmen, S. and Schreiber, K.-F. (2002) Comparison of species composition between different grassland management treatments after 25 years. *Applied Vegetation Science*, 5, 99–106. https://doi.org/10.1111/j.1654-109X.2002.tb00539.x

Mucina, L., Bültmann, H., Dierßen, K., Theurillat, J.-P., Raus, T., Čarni, A. et al. (2016) Vegetation of Europe: hierarchical floristic classification system of vascular plant, bryophyte, lichen, and algal communities. *Applied Vegetation Science*, 19, 3–264. https://doi.org/10.1111/avsc.12257

Münzbergová, Z. and Herben, T. (2004) Identification of suitable unoccupied habitats in metapopulation studies using co-ocurrence of species. *Oikos*, 105, 408–414.

Murren, C.J. (2002) Phenotypic integration in plants. *Plant Species Biology Plant Species Biology*, 17, 89–99. https://doi.org/10.1046/j.1442-1984.2002.00079.x

Newbold, T. (2018) Future effects of climate and land-use change on terrestrial vertebrate community diversity under different scenarios. *Proceedings of the Royal Society B-Biological Sciences*, 285, 20180792. https://doi.org/10.1098/rspb.2018.0792

Noy-Meir, I. and van der Maarel, E. (1987) Relations between community theory and community analysis in vegetation science: some historical perspectives. *Vegetatio*, 69, 5–15.

Omelka, M. and Hudecová, Š. (2013) A comparison of the Mantel test with a generalised distance covariance test. *Environmetrics*, 24, 449–460. https://doi.org/10.1002/env.2238

Pillar, V.D., Duarte, L.S., Sosinski, E.E. and Joner, F. (2009) Discriminating trait-convergence and trait-divergence assembly patterns in ecological community gradients. *Journal of Vegetation Science*, 20, 334–348. https://doi.org/10.1111/j.1654-1103.2009.05666.x

Pillar, V.D. (1999) On the identification of optimal plant functional types. *Journal of Vegetation Science*, 10, 631–640.

Pillar, V.D. and Orloci, L. (1993) *Character-Based Community Analysis; the Theory and an Application Program*. SPB Academic Publishing.

Poschlod, P. and WallisDeVries, M.F. (2002) The historical and socioeconomic perspective of calcareous grasslands—lessons from the distant and recent past. *Biological Conservation*, 104, 361–376. https://doi.org/10.1016/S0006-3207(01)00201-4

Regan, K.M., Nunan, N., Boeddinghaus, R.S., Baumgartner, V., Berner, D., Boch, S. et al. (2014) Seasonal controls on grassland microbial biogeography: Are they governed by plants, abiotic properties or both? *Soil Biology and Biochemistry*, 71, 21–30. https://doi.org/10.1016/j.soilbio.2013.12.024

Robert, P. and Escoufier, Y. (1976) A unifying tool for linear multivariate statistical methods: The RV-coefficient. *Applied Statistics*, 25, 257–265. https://doi.org/10.2307/2347233

Royer, J.M. (1991) Synthèse eurosibérienne, phytosociologique et phytogéographique de la classe des Festuco-Brometea. *Dissertationes Botanicae*, 178, 1–296.

Schrodt, F., Kattge, J., Shan, H., Fazayeli, F., Joswig, J., Banerjee, A. et al. (2015) BHPMF - a hierarchical Bayesian approach to gap-filling and trait prediction for macroecology and functional biogeography. *Global Ecology and Biogeography*, 24, 1510–1521. https://doi.org/10.1111/geb.12335

Shan, H., Kattge, J., Reich, P., Banerjee, A., Schrodt, F., and Reichstein, M. (2012) Gap Filling in the Plant Kingdom - Trait Prediction Using Hierarchical Probabilistic Matrix Factorization. In: Langford, J. (Ed.) *Proceedings of the International Conference for Machine Learning (ICML)*. Edinburgh: International Conference on Machine Learning, pp. 1303–1310.

Siefert, A.,, Violle, C., Chalmandrier, L., Albert, C.H., Taudiere, A., Fajardo, A. et al. (2015) A global meta-analysis of the relative extent of intraspecific trait variation in plant communities. *Ecology Letters*, 18, 1406–1419. https://doi.org/10.1111/ele.12508

Sih, A. and Gleeson, S.K. (1995) A limits-oriented approach to evolutionary ecology. *Trends in Ecology & Evolution*, 10, 378–382. https://doi.org/10.1016/S0169-5347(00)89142-9

Smith, R.J. (2017) Solutions for loss of information in high-beta-diversity community data. *Methods in Ecology and Evolution*, 8, 68–74. https://doi.org/10.1111/2041-210X.12652

ter Braak, C.J.F., Peres-Neto, P.R. and Dray, S. (2018) Simple parametric tests for trait–environment association. *Journal of Vegetation Science*, 29, 801–811. https://doi.org/10.1111/jvs.12666

Thomson, J.D., Weiblen, G., Thomson, B.A., Alfaro, S. and Legendre, P. (1996) Untangling multiple factors in spatial distributions: lilies, gophers, and rocks. *Ecology*, 77, 1698–1715. https://doi.org/10.2307/2265776

Violle, C., Navas, M.-L., Vile, D., Kazakou, E., Fortunel, C., Hummel, I. et al. (2007) Let the concept of trait be functional!. *Oikos*, 116, 882–892. https://doi.org/10.1111/j.2007.0030-1299.15559.x

Willner, W., Roleček, J., Korolyuk, A., Dengler, J., Chytrý, M., Janišová, M. et al. (2019) Formalized classification of semi-dry grasslands in central and eastern Europe. *Preslia*, 91, 25–49. https://doi.org/10.23855/preslia.2019.025

Wilson, J.B. (2007) Trait-divergence assembly rules have been demonstrated: Limiting similarity lives! A reply to Grime. *Journal of Vegetation Science*, 18, 451–452.

Wilson, J.B., Weiher, E. and Keddy, P.A. (1999) *Assembly Rules in Plant Communities*. Cambridge University Press, pp. 130–164.

Wright, I.J., Reich, P.B., Westoby, M., Ackerly, D.D., Baruch, Z., Bongers, F. et al. (2004) The worldwide leaf economics spectrum. *Nature*, 428, 821–827. https://doi.org/10.1038/nature02403

Zelený, D. (2018) Which results of the standard test for community-weighted mean approach are too optimistic? *Journal of Vegetation Science*, 29, 953–966. https://doi.org/10.1111/jvs.12688

Zelený, D. and Schaffers, A.P. (2012) Too good to be true: pitfalls of using mean Ellenberg indicator values in vegetation analyses. *Journal of Vegetation Science*, 23, 419–431. https://doi.org/10.1111/j.1654-1103.2011.01366.x

SUPPORTING INFORMATION

Additional supporting information may be found online in the Supporting Information section.

Appendix S1. Parameters set for the simulation of metacommunities used for the analyses shown in Figure 2 and summary diversity statistics

Appendix S2. Location of the grassland plots of the GVRD dataset used in Willner et al. (2019)

Appendix S3. Traits used for the analysis of dry calcareous grassland communities

Appendix S4. Proportion of significant Rd correlation *r*(**XY**) across simulated metacommunities under Scenario 2

Appendix S5. Proportion of significant Rd correlation *r*(**XY**) across simulated metacommunities under Scenario 4

Appendix S6. Proportion of significant Rd correlations *r*(**XW**) and *r*(**XE**) across metacommunities simulated under Scenario 1

Appendix S7. Effect of sample size on power of Rd correlations *r*(**XY**) and *r*(**XW**)

Appendix S8. Frequency distributions of proportional beta diversity and Rd correlations *r*(**WE**) and *r*(**YE**) across metacommunities simulated under Scenario 1

Appendix S9. Numerical results for best solutions shown in Figure 5

Appendix S10. Biplot of principal components analysis (PCA) of the species on the basis of the matrix of species by the traits found relevant in community assembly (Figure 5)

Appendix S11. Pearson correlation matrices between traits at species level

Appendix S12. Pearson correlation matrices between CWMs at community level

Appendix S13. Principal components analysis (PCA) of dry grassland plots based on the fuzzy-weighted composition

Appendix S14. Pearson correlation coefficients between principal components of Beals' smoothed composition and fuzzy-weighted composition, community-weighted means (CWMs) and environmental variables

Appendix S15. Principal component analysis of dry grassland plots based on Beals' smoothed composition, showing the species

Appendix S16. Species found in dry calcareous grassland relevés extracted from the GVRD database

Appendix S17. Identification numbers of the relevés extracted from the GVRD database

How to cite this article: Pillar VD, Sabatini FM, Jandt U, Camiz S, Bruelheide H. Revealing the functional traits linked to hidden environmental factors in community assembly. *J Veg Sci*. 2020;00:e12976. https://doi.org/10.1111/jvs.12976